Wave-Based Turing Machine: Time Reversal and Information Erasing

S. Perrard,[1,*] E. Fort,[2] and Y. Couder[1]
[1]Laboratoire Matière et Systèmes Complexes, Université Paris Diderot, CNRS UMR 7057, Bâtiment Condorcet, 10 rue Alice Domon et Léonie Duquet, 75013 Paris, France
[2]Institut Langevin, ESPCI Paris, PSL Research University, CNRS UMR 7587, 1 rue Jussieu, 75238 Paris, France
(Received 17 January 2016; revised manuscript received 20 June 2016; published 26 August 2016)

The investigation of dynamical systems has revealed a deep-rooted difference between waves and objects regarding temporal reversibility and particlelike objects. In nondissipative chaos, the dynamic of waves always remains time reversible, unlike that of particles. Here, we explore the dynamics of a wave-particle entity. It consists in a drop bouncing on a vibrated liquid bath, self-propelled and piloted by the surface waves it generates. This walker, in which there is an information exchange between the particle and the wave, can be analyzed in terms of a Turing machine with waves as the information repository. The experiments reveal that in this system, the drop can read information backwards while erasing it. The drop can thus backtrack on its previous trajectory. A transient temporal reversibility, restricted to the drop motion, is obtained in spite of the system being both dissipative and chaotic.

DOI: 10.1103/PhysRevLett.117.094502

In physics, time reversal symmetry, i.e., the invariance of the dynamical equations under the transformation $t \to -t$, is a general property of conservative systems. But, there is a widely studied fundamental difference [1] in the temporal reversibility of waves and particles. For waves, temporal reversibility is preserved even in the presence of chaos. This yields surprising possibilities as observed in optical phase conjugation [2], time-reversed acoustics [3,4], microwaves [5], elastic waves [6], or surface waves [7,8]. For particles, as demonstrated in, e.g., billiards, the temporal reversibility is destroyed in the chaotic regimes by the sensitivity to initial conditions.

Is time reversibility restored for a particle dynamics when it is piloted by a wave? In the present work, we investigate this question experimentally using a walker, a dynamical entity associating a drop bouncing on a vertically oscillating bath with the waves it generates [9–14]. We first show that an imposed phase shift between the bouncing motion and the surrounding waves leads naturally to a reversal of the instantaneous drop velocity. Surprisingly, in chaotic regimes, the same phase shift leads not only to a reversal of the instantaneous velocity, but also to a reversal of the motion along complex trajectories. This is equivalent to a temporal reversibility, unexpected in a system both dissipative and chaotic. We show that this property emerges from a dynamical erasing process of the pregenerated wave field. Eventually, we revisit the dynamics of these walkers in terms of writing, storing, reading, and erasing processes. We show that this system implements the basic elements of a Turing machine using standing waves as a global information repository.

Walkers are obtained in the experimental setups usually devoted to the study of the Faraday instability [15]. A bath of silicon oil of viscosity $\nu = 2 \times 10^{-2}$ Pas is oscillated vertically with an acceleration $\gamma(t) = \gamma_m \cos(2\pi f_0 t)$ and a frequency $f_0 = 80$ Hz. When the imposed oscillating acceleration exceeds a threshold $\gamma_F \approx 4.5g$, waves appear spontaneously at the bath surface. These are parametrically forced Faraday standing waves oscillating at half the forcing frequency: $f_F = f_0/2$ [16]. Below but close to the Faraday instability threshold ($4g < \gamma_m < \gamma_F$), a drop of typical diameter $D = 600$ μm of the same oil is observed to bounce at half the forcing frequency $f_W = f_0/2$. Correlatively, the drop excites damped Faraday waves [11]. In this regime, the drop becomes propelled by its interaction with the waves it emits. At each collision with the bath, the drop receives a kick in a direction determined by the local slope of the interface. The resulting wave-induced force can be written $\vec{F}_m = -C\vec{\nabla}h$, where C is a coupling constant and $\vec{\nabla}h$ is the surface height gradient evaluated at the impact point [10]. It leads to a propelled motion at a velocity $V_0 \approx 10$ mm/s.

As sketched in Fig. 1, the drop vertical motion being subharmonic, it can have two different phases relative to the forcing oscillation. Having chosen arbitrarily an origin of time, we can distinguish odd and even periods of the forcing [respectively labeled A and B in Fig. 1(a)]. In normal conditions, the bouncing is strictly subharmonic so that a given drop hits the surface during either the A or the B periods. The emitted waves are also subharmonic and temporally synchronized with the bouncing phase of the drop. An abrupt change of the drop bouncing from, e.g., phase A to phase B, therefore generates a π shift between the drop periodic motion and the preexisting wave. The π shift is induced by a brief and controlled disturbance of the forcing oscillation, as sketched in Fig. 1(a). The amplitude of the sinusoidal input $\gamma(t)$ is increased from γ_m to $\gamma_m + \Delta\gamma_m$ during two periods T_0 of the bath oscillation. Regardless of the bouncing phase, the drop receives one

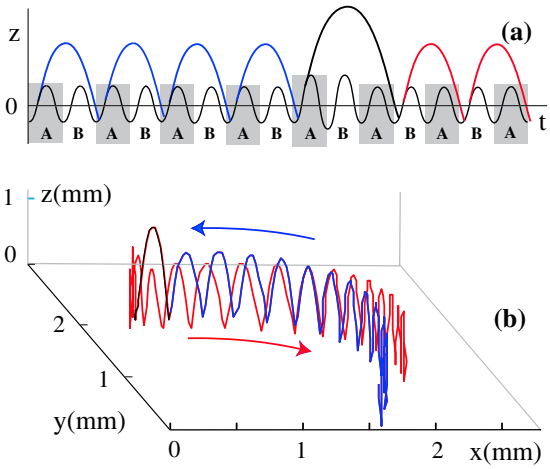

FIG. 1. (a) Sketch of the time evolution of both the vertical position of the bath (solid black line) and the drop position. On the left, the drop bounces on the surface during periods A of the forcing oscillation (solid blue line). A π shift is induced by a transient increase of the imposed oscillation, after which the drop bounces during periods B (solid red line). (b) A real droplet trajectory as seen in perspective, reconstructed by particle tracking from a zoomed-in high-speed movie before (blue line), during (black line), and after (red line) the π shift.

single vertical kick of larger amplitude. For $\Delta\gamma_m = (0.45 \pm 0.02)\gamma_m$, the resulting free flight of the drop lasts three periods instead of two. After this anomalous jump, the drop bouncing phase is thus π shifted as compared to the waves generated before the disturbance. These waves are practically undisturbed by the forcing amplitude anomaly. The drop thus collides with an opposed wave field $h \to -h$ so that the horizontal component of the kick is reversed. Figure 1(b) shows in perspective the detail of the drop motion, as reconstructed from a fast camera recording at 800 fps and synchronized with the bath acceleration. The transient increase of the free flight height (solid black line) induces a π shift in the bouncing phase, as expected. The reversal of the drop velocity is not necessarily instantaneous since it is very sensitive to the time of the first anomalous landing. In the case shown in Fig. 1(b), three vertical bounces are observed before reversal. The reversal duration δt_π lasting $0 < \delta t_\pi < 0.12$ s has no visible influence on the accuracy of the later backtrack motion since $V\delta t_\pi \ll \lambda_F$.

The possibility of imposing abruptly a π shift provides a tool to investigate a motion reversal in a memory-endowed regime. The walker's memory [11] is due to the persistence of the standing waves partly sustained by Faraday forcing. In the vicinity of the Faraday instability threshold γ_F, each impact of the drop on the bath generates a localized mode of Faraday standing waves of wavelength $\lambda_F = 4.75$ mm that can be approximated by a circular Bessel function J_0 centered at the collision point [11]. Since these waves are partly sustained by the vertical forcing, each Bessel wave decays slowly on a time scale τ determined by the relative distance to the Faraday instability threshold $\tau \approx T_F\gamma_F/(\gamma_F - \gamma_m)$.

The global field results from the linear addition of standing waves previously created by $\mathrm{Me} = \tau/T_F$ sources distributed along the droplet recent trajectory. The resulting global interference pattern thus contains a memory of the followed path. In the present experimental setup, Me can be tuned from 5 to approximately 200 by varying γ_m.

Whenever the walker's motion is spatially confined, the effect of memory was found to be determinant, leading to stable or chaotic trajectories. In order to test the temporal reversibility on various types of trajectories, we use a well-documented experiment in which a walker is trapped in a 2d harmonic potential well of characteristic pulsation ω [17,18]. The confinement is achieved by using drops loaded with ferrofluid immersed in an axisymmetric magnetic field gradient. In the short memory regimes, the trajectories are circular and reversed by the velocity reversal. For long memories ($\mathrm{Me} > 50$), two regimes arise depending on the width of the harmonic potential well $\Lambda = V_0/\lambda_F\omega$.$\Lambda$ measures the mean extension of the drop trajectory in units of the Faraday wavelength λ_F. In the narrow band of values of $\Lambda \approx \Lambda_{n,m}$, the walker follows stable deterministic trajectories that can be in the shape of, e.g., a circle, a lemniscate, or a trifolium, with a quantization of the orbit size level n and angular momentum level m [17]. In all these cases, after the π shift, the wave-guided drop turns back and follows the same orbit in reverse [see Figs. 2(a) and 2(b)]. This means that the walker angular momentum changes sign as expected from a time reversal.

We then turn to unsteady situations by choosing a value of the confining parameter Λ that does not correspond to any stable orbit. In this case, the trajectory is chaotic in the sense of having a hypersensitivity to initial conditions. A previous study has shown that the system is, however, still deterministic with a small number of degrees of freedom involved in spite of the complexity of both the drop trajectory and the surrounding wave field [18]. After an imposed phase shift, the drop is observed to return on its track, following in reverse its complex past trajectory, as shown in the two examples of Figs. 2(c) and 2(d). Experiments performed for various values of the memory ranging from $\mathrm{Me} = 40$ to $\mathrm{Me} = 150$ reveal that the typical time of divergence increases with increasing memory parameter. A dispersion of the divergence times is, however, observed for each memory. In order to obtain quantitative results, we perform statistical measurements on the correlation between the initial and the reversed motion.

The drop trajectory is recorded during long-lasting experiments with repeated π-shifts events equally spaced in time with a periodicity of 10 s. This duration is longer than the observed correlation times between the forward and the backward paths. The times t_π of π shift events are singled out using image processing and the known periodicity of the imposed phase shifts. The correlation between

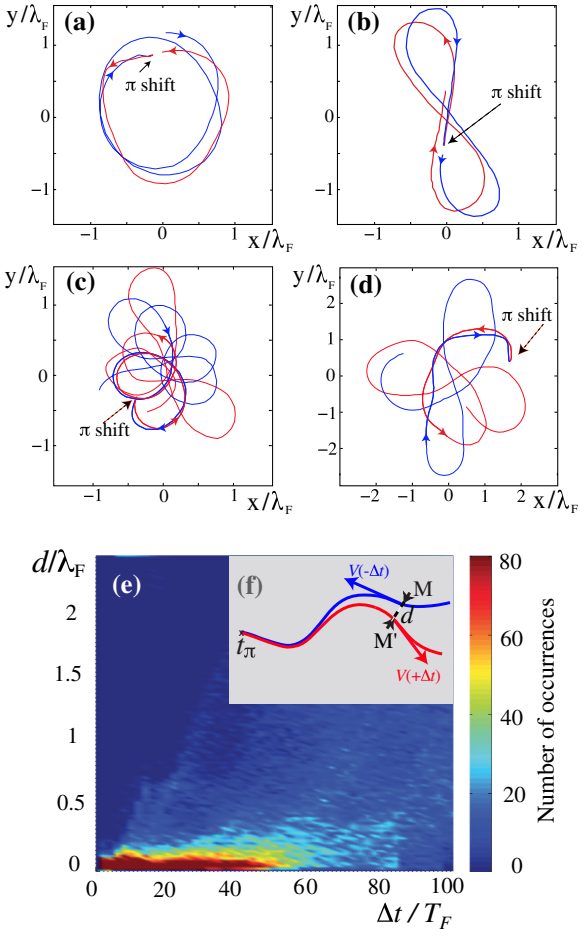

FIG. 2. Trajectories observed before (solid blue line) and after a π shift (solid red line) for various types of orbital motions. (a) Stable circular orbit observed for $\mathrm{Me} = 100$ and $\Lambda = \Lambda_{2,2} = 0.9$. (b) Stable lemniscate observed at $\mathrm{Me} = 100$ and $\Lambda = \Lambda_{2,0} = 0.75$. (c),(d) Chaotic regimes for $\mathrm{Me} = 70$, $\Lambda = 0.49$ and $\mathrm{Me} = 180$, $\Lambda = 0.82$. In the two latter cases, the drop motion is reversed on a trajectory length of the order of $\delta/2 = V_0 \mathrm{Me} T_F/2$. (e) Histogram of the temporal evolution of the distance $d(t)$ [as defined in (f)] of the drop position at two times symmetrical with respect to the time t_π of the phase shift. This color-coded histogram was obtained from $N = 250$ trajectories. Time is expressed in number of bounces.

the forward and the backward motions is then measured from the distance d between the droplet positions at two times symmetrical with respect to the π shift $d(\Delta t)$, as sketched in Fig. 2(f). A histogram of the distances $d(\Delta t)$ is plotted in Fig. 2(e) as a function of the elapsed time Δt from the π shift. The distances d remain small during a time Δt of the order of $\mathrm{Me}/2$ for all the imposed π shift. Control experiments have then been done using the same experimental parameters but without performing any π shift. The observed motion is a highly chaotic trajectory. This chaos had been investigated using a Poincaré return map [18]. In this regime, two trajectories with neighboring initial conditions diverge from each other. In contrast, a π shift forces the drop to return on a predetermined trajectory so that during a finite time, the motion is reversed, even though the dynamics is dissipative. It is the first observation of an effect theoretically predicted by Devaney [19] that a dynamical system (not necessarily conservative) is reversible if there exists a transformation G in phase space that reverses the direction of time and is also an involution (i.e., G composed with itself yields identity). In the present study, a π shift is such an involution of the current dynamics. In the very high memory limit ($\mathrm{Me} \approx 150$), the motion of a walker is affected by fluctuations of its velocity modulus. They appear to be a hindrance to a further increase of the reversibility time.

An insight into this time reversal phenomenon is provided by investigating the wave field. It can be recorded as seen from above at 800 fps with a fast camera phase locked on the bath oscillations. The effect of the π shift on the wave field is best observed by extracting from these recordings two films at half the forcing frequency and corresponding to two observations strobed in phases A and B, respectively (see Supplemental Material 1 [20]). Figures 3(a) and 3(b) show two instantaneous wave fields observed when the drop is moving (a) forward and (b) backward, respectively. During its initial motion, the bouncing of the drop builds up a wave field. It can be observed by comparing Figs. 3(a) and 3(b) that the whole wave field associated with the return motion seems to be of smaller amplitude than that of the forward motion. This effect can be analyzed quantitatively by computing the wave field from the drop trajectory [11] (see detail in Supplemental Material 2 [20]). The surface height at time t in position $\vec{\rho}$ is given by

$$h(\vec{\rho},t) = h_0 \sum_{t_n > t_\pi} J_0(k_F||\vec{\rho} - \vec{r}(t_n)||) e^{-(t-t_n)/(\mathrm{Me}T_F)} - h_0 \sum_{-\infty < t_n < t_\pi} J_0(k_F||\vec{\rho} - \vec{r}(t_n)||) e^{-(t-t_n)/(\mathrm{Me}T_F)}, \quad (1)$$

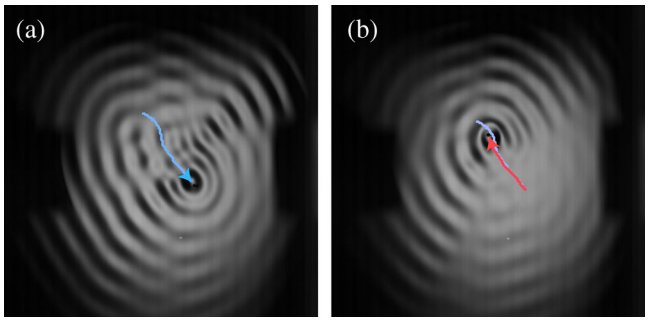

FIG. 3. Direct visualisation of the wave field observed during the (a) forward and the (b) backward motion of the drop. The forward (blue arrow) and backward (red arrow) trajectories have been superimposed.

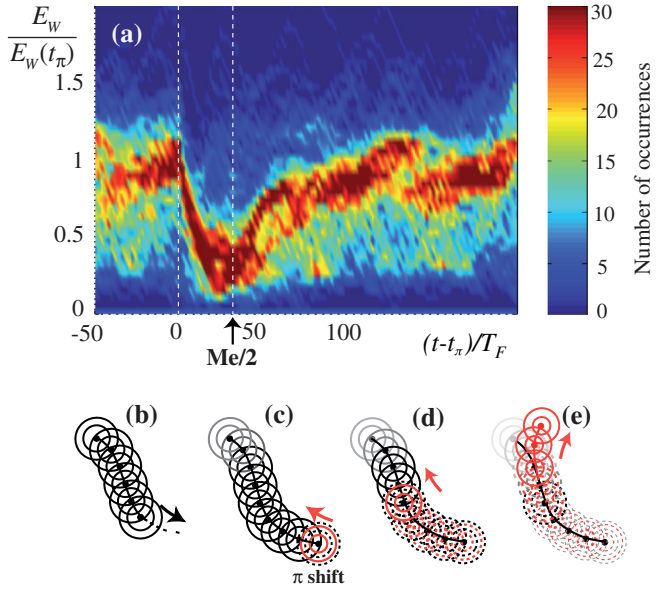

FIG. 4. Characterization of the wave erasing process. (a) Histogram of the wave energy $E_W/E_W(t_\pi)$ as a function of time computed using Eqs. (1) and (2) for 324 experimental trajectories obtained for $\mathrm{Me} = 70 \pm 15$ and $\Lambda = 0.63 \pm 0.02$, each having undergone a π shift event. The origin of time is taken at the π shift, and the wave energy is normalized by its value at this time. (b)–(e) Sketches of the wave field buildup. (b) During the initial forward motion. (c) At the π shift. (d) During the backward motion corresponding to an erasing process that results from the phase opposition between the old waves (black circles) and the new ones (red circles). The dashed circles symbolize the wave destruction by interferences. (e) The drop no longer backtracks and starts forming a new field.

where h_0 is the initial amplitude of wave and $\vec{r}(t_n)$ is the impact position at time t_n. Before and after t_π, the wave sources only differ from a phase π. Therefore, during the backward motion, each bounce emits a wave of opposite phase that interfere with the previously generated waves. A quantitative measurement of this phenomenon is obtained from an analysis of the normalized global energy of the wave field [13]:

$$E_W(t) = \frac{1}{h_0^2} \iint [h(\vec{\rho}, t)]^2 dS / \iint [J_0(\vec{\rho}, t)]^2 dS, \qquad (2)$$

where E_W has been normalized by the energy of a single impact source J_0. Figure 4(a) shows the histogram of the evolution of $E_W/E_W(t_\pi)$ as a function of time before and after a π shift taken as the origin of time. It has been computed from 324 trajectories obtained at $\mathrm{Me} = 70 \pm 15$. After the π shift, the total energy $E_W/E_W(t_\pi)$ is observed to decrease down to 0.35 of its initial value. This minimum is reached at a time t approximately equal to $\mathrm{Me}/2$. It corresponds to the period of time during which the droplet backtracks. As sketched in Figs. 4(c) and 4(d), the new emitted waves have a phase opposite to the initial ones so that they erase step by step the previous wave field. The new wave being more recent has an amplitude that exceeds that of the old one by an exponential factor $e^{-2(t-t_\pi)}$. This effect grows in time, and for times larger than $\mathrm{Me}/2$, a new wave field is generated and the trajectory diverges again.

The first and main result is that the availability of intrinsic recorded information about the past can make a temporal reversibility possible for an elementary system even in dissipative and chaotic conditions. Our second result is the finding of a wave erasing process. It gives strength to the description of walker dynamics as an implementation of an iterative computing process. The internal clock is here provided by the periodicity T_F of the Faraday waves and the vertical bouncing motion. At each drop bounce, the generation of a standing Bessel wave can be interpreted as a *writing* process by which the drop encodes positional information in an extended wave field. Because of the parametric forcing of this wave field, the positional information is maintained for a given time, which corresponds to a *storing* process in a wave field. At each new bounce, the drop as it comes in close contact with the bath receives a horizontal kick proportional to the local slope. It corresponds to a *reading* process in which the stored information determines the drop's next jump. To these three basic operations (writing, storing, and reading), we have added the existence of the fourth basic elementary operation: the *erasing* process, which can be here triggered by an imposed π shift on the bouncing phase of the drop. The specificity and the associated richness of this iterative machine rely here on the way the information is written, stored, and processed. Each individual positional information is stored in a global wave field, submitted to the superposition principle of waves. The walker can in that sense be termed as a wave Turing machine. With the present control of the bouncing phase, the wave memory can be written or erased on demand. This dynamical information storage through a global wave memory can thus be controlled. Even though the present system is unpractical, the finding of similar coupling with waves of a different nature could lead to computing possibilities.

The authors thank M. Labousse and Y. Pomeau for useful discussions, S. Neveu for providing us the ferrofluid we used, and D. Charalampous, A. Lantheaume, and L. Rhéa for technical assistance. This work was supported by the French government through Grants No. ANR-11-BS04-001-01, No. ANR-10-IDEX-0001-02 PSL*, and No. ANR-10-LABX-24, and by the AXA Research Fund.

*Corresponding author.
sperrard@uchicago.edu
Present address: James Franck Institute, University of Chicago, 929 East 57th Street, Chicago, Illinois 60637, USA.

[1] R. K. Snieder and J. A. Scales, Phys. Rev. E **58**, 5668 (1998).

[2] B. Zeldovich, N. F. Pilipetsky, and V. V. Shkunov, *Principles of Phase Conjugation* (Springer-Verlag, Berlin, 1985).
[3] A. Derode, P. Roux, and M. Fink, Phys. Rev. Lett. **75**, 4206 (1995).
[4] M. Fink and C. Prada, Inverse Probl. **17**, R1 (2001).
[5] G. Lerosey, J. de Rosny, A. Tourin, A. Derode, and M. Fink, Appl. Phys. Lett. **88**, 154101 (2006).
[6] C. Draeger and M. Fink, Phys. Rev. Lett. **79**, 407 (1997).
[7] J. A. G. Roberts and G. R. W. Quispel, Phys. Rep. **216**, 63 (1992).
[8] V. Bacot, M. Labousse, A. Eddi, M. Fink, and E. Fort, Nat. Phys. (2016).
[9] Y. Couder, S. Protiere, E. Fort, and A. Boudaoud, Nature (London) **437**, 208 (2005).
[10] S. Protiere, A. Boudaoud, and Y. Couder, J. Fluid Mech. **554**, 85 (2006).
[11] A. Eddi, E. Sultan, J. Moukhtar, E. Fort, M. Rossi, and Y. Couder, J. Fluid Mech. **674**, 433 (2011).
[12] A. U. Oza, R. R. Rosales, and J. W. M. Bush, J. Fluid Mech. **737**, 552 (2013).
[13] C. Borghesi, J. Moukhtar, M. Labousse, A. Eddi, E. Fort, and Y. Couder, Phys. Rev. E **90**, 063017 (2014).
[14] J. W. M. Bush, Annu. Rev. Fluid Mech. **47**, 269 (2015).
[15] S. Douady, J. Fluid Mech. **221**, 383 (1990).
[16] T. Benjamin and F. Ursell, Proc. R. Soc. A **225**, 505 (1954).
[17] S. Perrard, M. Labousse, M. Miskin, E. Fort, and Y. Couder, Nat. Commun. **5**, 3219 (2014).
[18] S. Perrard, M. Labousse, E. Fort, and Y. Couder, Phys. Rev. Lett. **113**, 104101 (2014).
[19] R. L. Devaney, Trans. Am. Math. Soc. **218**, 89 (1976).
[20] See Supplemental Material at http://link.aps.org/supplemental/10.1103/PhysRevLett.117.094502 for two movies of the dynamics before, during and after a pi shift (Supp1) as well as a description of the numerical method used to compute the wave field (Supp2).